ISSN 1028-334X, Doklady Earth Sciences, 2021, Vol. 501, Part 1, pp. 933–937. © Pleiades Publishing, Ltd., 2021.
Russian Text © The Author(s), 2021, published in Doklady Rossiiskoi Akademii Nauk. Nauki o Zemle, 2021, Vol. 501, No. 1, pp. 43–48.

VOLCANOLOGY

The Structure of the Upper Crust beneath the Kambalny Volcano (South Kamchatka) Revealed from Ambient Noise Tomography

N. N. Belovezhets[a,b,*], Y. M. Berezhnev[a,b], Corresponding Member of the RAS I. Yu. Koulakov[a,b,c], N. M. Shapiro[d,e], I. F. Abkadyrov[c], S. N. Rychagov[c], and Academician E. I. Gordeev[c]

Received July 21, 2021; revised July 22, 2021; accepted July 22, 2021

Abstract—The result of ambient noise tomography for the Kambalny Volcano (South Kamchatka), where the first time in the entire history of observations a violent phreatic eruption was observed in March–April 2017, is presented. The results obtained clarify the structure of the upper part of the edifice of the Kambalny Volcano and are consistent with independent data on body waves, as well as with geological information. According to seismotomographic data of the surface waves, low-velocity anomalies are distinguished in the model of the structure of the volcanic edifice. They are asymmetric relative to the volcano cone and are allocated to loose pyroclastic deposits of past eruptions and to deep sources of hydrothermal activity. Perhaps the migration of fluids in these hydrothermal vents to the north and west of the volcano and their interaction with the magma chamber in the upper crust caused the explosive eruption.

Keywords: seismic noise, surface waves, ambient noise tomography, upper crust, velocity anomalies, Kamchatka, Kambalny Volcano

DOI: 10.1134/S1028334X21110040

Kambalny is the southernmost stratovolcano of the Holocene Age on the Kamchatka Peninsula. Data on its historical eruptions were absent until recently, so it was assigned to dormant volcanoes. The age of the youngest pyroclastic flows was estimated at about 600 years [18]. An eruption of the Kambalny Volcano unexpectedly began on March 25, 2017, and was accompanied by intensive seismicity [5] and strong gas emission [1]. The first explosion threw out a cloud of gas and ash to a height of more than 5–6 km [1]. After that, the plume of the eruption was spread southward over a distance of about 1000 km in one day and created a particular risk for air transport in the region [1]. Through mid-April 2017, several other explosions occurred, some of which exceeded the force of the first one. After that, the eruption gradually ended, and further activity of the Kambalny Volcano consisted in moderate fumarole emission, which lasted several months. Lava flows and any traces of the release of juvenile material were not seen during this eruption, and therefore it was concluded that it was phreatic [4].

The Kambalny Volcano is located at the edge of the submeridional Kambalny Ridge, which is defined as a Middle-Upper Quaternary tectonic-magmatic uplift in the Pauzhetka volcanotectonic depression [6]. The edifice of the volcano consists of mafic rocks: alternating slag-like and massive basalts, agglomerate lavas, and pyroclastic deposits [8]. The volume of pyroclastic deposits on the Kambalny Volcano is about twice as large as the lava flows, which is typical for basalt stratovolcanoes [18]. The crater at the volcano top is 750 × 550 m in size, to 150 m deep, and is opened to the southwest. An explosion funnel 10–50 m deep and 200 × 100 m in size adjoins the crater to the southeast of the summit. These structures of Late Holocene age were formed as a result of one or several directional explosions [4]. During the recent eruption in 2017, a sink-funnel 115 × 100 m was formed near the summit.

There are many areas of hydrothermal activity in the vicinity of the Kambalny Volcano that are assigned to the most significant on Kamchatka. The Pauzhetka geothermal field is the most well-known among them; it is located 20 km to the southwest of the volcano, and the first geothermal power plant in the Soviet Union was built there [7]. Strong thermal phenomena, which are also considered highly promising for industrial

[a] *Trofimuk Institute of Petroleum Geology and Geophysics, Siberian Branch, Russian Academy of Sciences, Novosibirsk, 630090 Russia*
[b] *Novosibirsk State University, Novosibirsk, 630090 Russia*
[c] *Institute of Volcanology and Seismology, Far East Branch, Russian Academy of Sciences, Petropavlovsk-Kamchatsky, 683006 Russia*
[d] *Schmidt Institute of Physics of the Earth, Russian Academy of Sciences, Moscow, 123995 Russia*
[e] *Centre National de la Recherche Scientifique, Université Grenoble Alpes (UGA), Grenoble, France*
**e-mail: BelovezhetsNN@ipgg.sbras.ru*

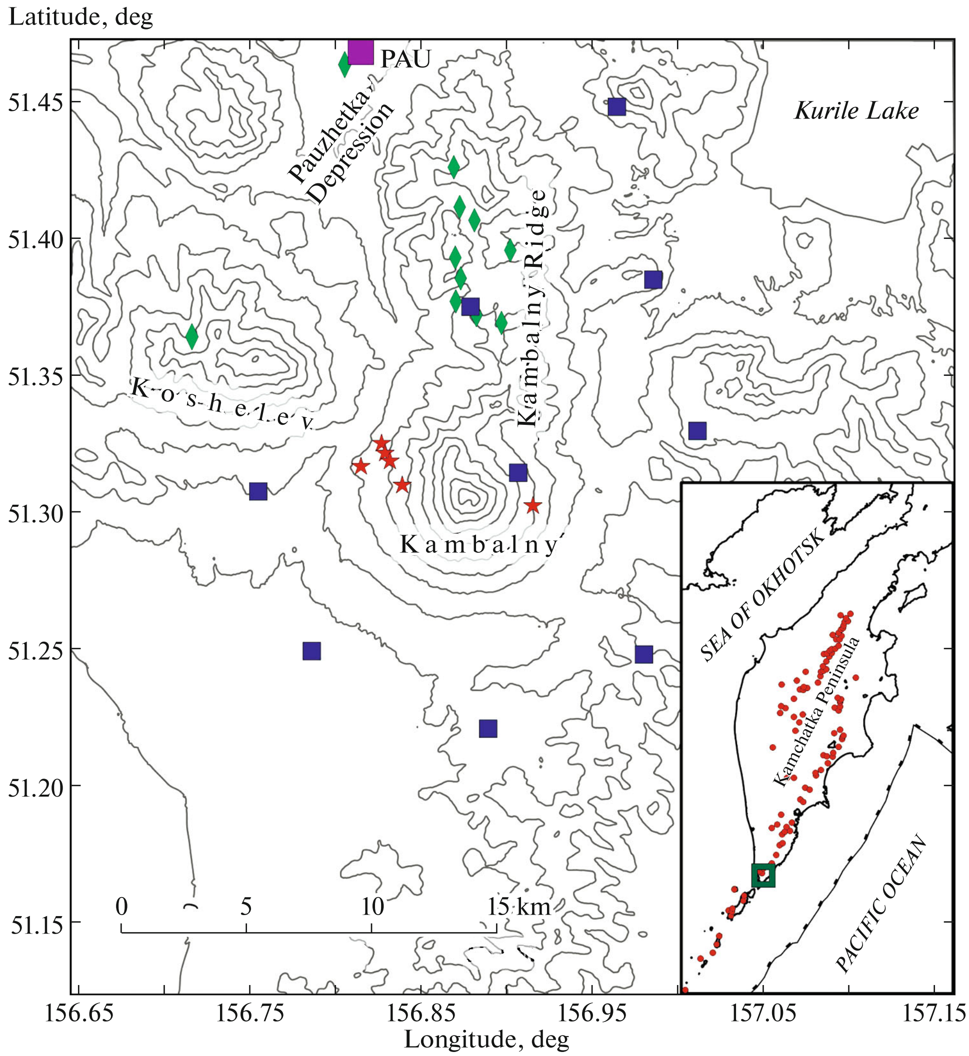

Fig. 1. The area around the Kambalny Volcano. The topography is shown by 200-m isolines, the purple square is the permanent Pauzhetka station; and the blue squares show the stations of the temporary network deployed in 2018–2019. Green diamonds are areas of geothermal activity, and red stars are monogenic cones. The inset reflects the position of the research area (green square) and volcanoes of Kamchatka (red dots).

use, are also seen in the area of the Koshelev Volcano to the west of the Kambalny Volcano. Another area of increased geothermal activity exists in the northern part of the Kambalny Ridge [3].

Until recently, the geophysical characteristics of the Kambalny Volcano and the adjacent area were insufficiently studied due to the remoteness and inaccessibility of this region. There is only one permanent seismic station Pauzhetka (PAU) in this area at a distance of 22 km from the top of the volcano; other monitoring stations are located at distances of more than 100 km. In this regard, the process of seismic activation during the eruption could not be determined in details. In order to study the local seismicity and to determine the deep structure under the volcano, a temporary seismic network, consisting of ten three-component broadband stations, was deployed on the slopes of the volcano and the surrounding area from July 2018 to July 2019 (Fig. 1). This article presents the first results of the study of the structure of the upper crust beneath the volcano obtained by ambient noise tomography.

Seismic ambient noise tomography is a relatively recent method [19], which has been intensively developed over the past 15 years and is now used to study geological structures at different scales [20]. In particular, it is regularly used to analyze near-surface layers in volcanic systems [11, 13, 15]. The general principle of this method consists in the fact that the cross-correlation of random seismic noise generated by sources uniformly distributed in space and recorded by two receivers converges to the Green function (the impulse response of the medium) between these two receivers [12]. Thus, the calculation of cross-correlations of

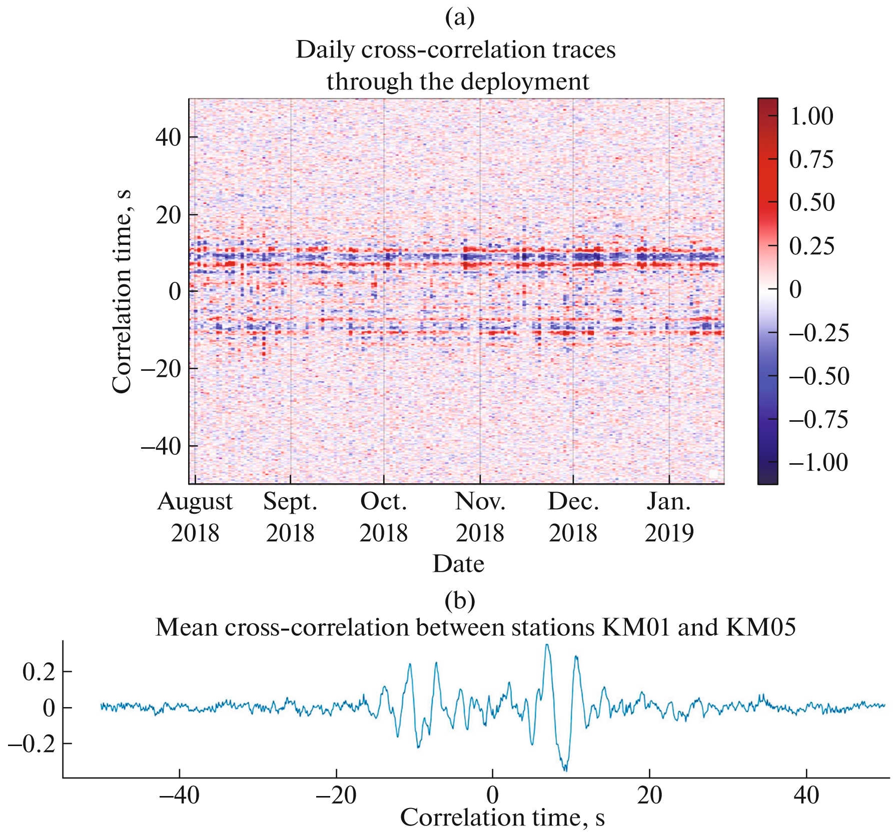

Fig. 2. (a) An example of computing cross-correlations for the pair of stations KM01 and KM05 in sliding windows and (b) the result of averaging for the entire observation period.

seismic noise may theoretically be used for the empirical synthesis of virtual point seismic sources located at the site of each of the receivers used. Taking into account the real properties of seismic noise recorded on the Earth's surface [9], volume seismic waves may be reconstructed from noise cross-correlations [16] only under particular favorable conditions. However, fundamental modes of surface waves may be easily reconstructed for almost all pairs of stations. Therefore, we use the most developed method of surface-wave noise tomography in our work [20].

The records of surface waves were detected in continuous seismic records according to the scheme proposed in [10]. Ocean waves of the Pacific Ocean and of the Sea of Okhotsk, as well as to a smaller degree of the Arctic Ocean, are the main noise sources. Data processing included prefiltering; removal instrumental response; removal of the mean, linear, and polynomial trends; and bandpass filtering in the 0.06–4 Hz window, resampling from 100 to 10 Hz, one-bit normalization, and spectral whitening with spectral windowing prior to and after normalization in the time domain. Then, the cross-correlation was computed in a sliding window of seismic records of vertical components for all pairs of stations available. An example of a time sweep of the correlation results from August 2018 to mid-January 2019 for one pair of stations (KM01–KM05) is shown in Fig. 2a. After that, the obtained values of the correlation function were averaged for the entire observation period, as shown for the selected pair of stations in Fig. 2b.

The obtained correlation functions are analogs of records of Rayleigh surface waves, traveling from one station to another. For these records, frequency–time analysis (FTAN) was conducted [14], which consisted in their filtration in a series of narrow sequential frequency bands. The determination of the maximum of the envelope curve by the received signals for each frequency provides dispersion curves reflecting the dependence of the group velocity of the Rayleigh wave on the frequency. Since the number of pairs of stations was small, the dispersion curves were manually constructed.

The distribution of the deep structure under the station network was constructed by the available dispersion curves based on the SURF_TOMO two-step surface wave tomography algorithm [17]. At the first stage, two-dimensional maps of group velocities for particular frequencies were constructed (Fig. 3) by performing several iterations, taking into account the curvature of rays on the seismic heterogeneities obtained. Then, a local dispersion curve was con-

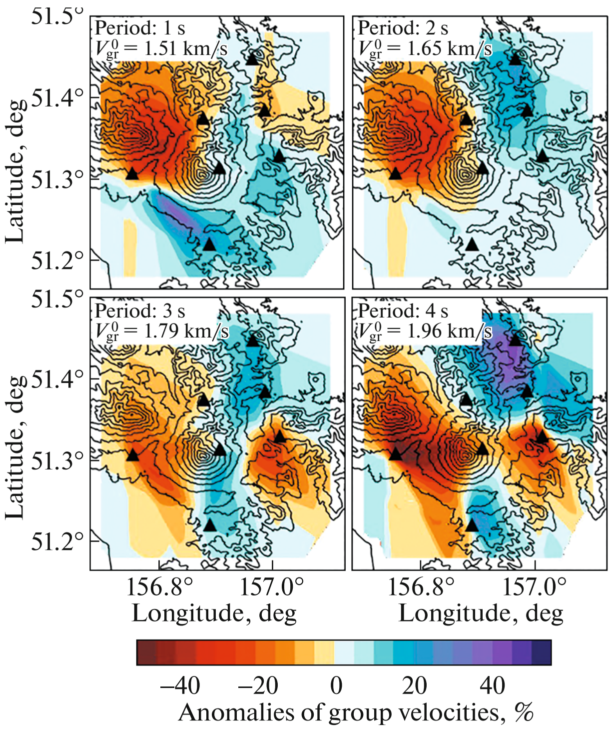

Fig. 3. Anomalies of the group velocities of the Rayleigh wave for periods of 1–4 s. Black triangles indicate seismic stations. The relief is reflected by 200-m isolines.

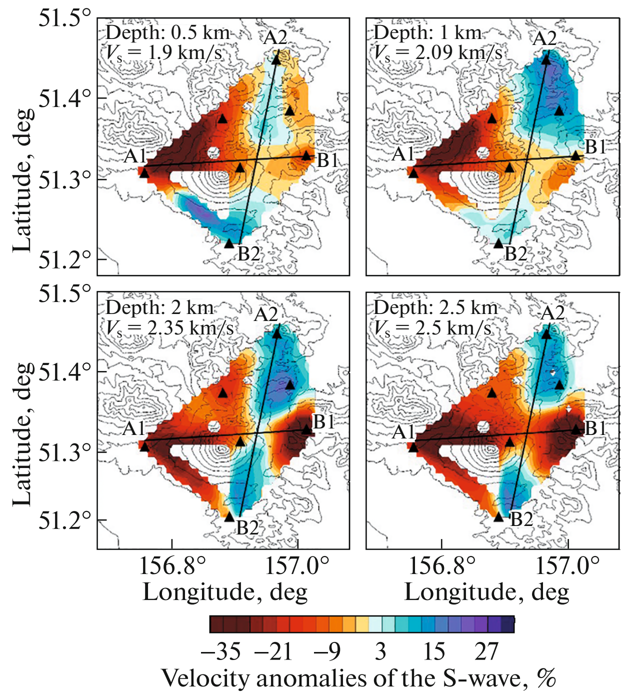

Fig. 4. Anomalies of S-wave velocities on four horizontal sections at depths from 0.5 to 2.5 km. Black triangles indicate seismic stations. The relief is shown by 200-m isolines.

structed at each point of the area, which was transformed into a one-dimensional distribution of the velocity of transverse waves (*Vs*) as a result of iterative linearized inversion. This procedure performed at all points of the area enabled us to construct a three-dimensional distribution of *Vs*, which is shown in Fig. 4 for four horizontal sections at depths from 0.5 to 2.5 km.

Unfortunately, the resolution of the tomographic model was not sufficiently high due to the small number of stations and low data density. Nevertheless, several synthetic tests performed show that the existing observation system enables the reconstruction of large anomalies with a change in sign in the area of the ridge and the summit of the Kambalny Volcano at a qualitative level. This in general corresponds to the results obtained after the inversion of the experimental data. It should also be pointed out that the distribution of velocity anomalies in this study corresponds at the qualitative level to the results obtained by the tomographic inversion of volume waves constructed by arrival times of waves of local seismicity.

The results obtained clarify the structure of the upper part of the edifice of the Kambalny Volcano and, in general, correspond to the geological data. The distribution of the group velocities of Rayleigh waves and of the velocities of S-waves is characterized by a segment of dominating low velocities to the south and west of the Kambalny Volcano. The negative anomaly with the greatest amplitude is located under the western slope of Kambalny and under the saddle in the direction towards the Koshelev Volcano. Low velocities there may correspond to deposits of slightly cemented pyroclastics, which accumulated during the eruptions of both volcanoes. They may also be explained by the presence of deep hydrothermal processes in the area between the two volcanoes, which are responsible for strong hydrothermal phenomena in the area of the Koshelev Volcano. It should be pointed out that the monogenic cones of the western slope of Kambalny are located above this low-velocity anomaly. It may be assumed that this anomaly is related to the upper part of the magma channel responsible for volcanic eruptions in the Holocene. In this case, the interaction of the magmatic body with meteoric waters is the factor of hydrothermal activity and of episodic phreatic eruptions of Kambalny, for example, of that in the spring of 2017.

A low-velocity anomaly was also determined to the north of the Kambalny Volcano along the Kambalny Ridge. It may be related to the distribution of geothermal sources in the upper crust, which form the large hydrothermal area of the Kambalny Volcano and the Pauzhetka field. The increased S-wave velocity in the western part of the stratovolcano and the Kambalny Ridge at depths of about 1 km and deeper are most likely allocated to the high-speed foundation composed of mafic rocks.

This article presents the first results of the study of the deep structure in the vicinity of Kambalny Volcano, a strong phreatic eruption of which occurred in 2017. Although the data on surface waves obtained by the cross-correlation of seismic noise cannot provide high resolution of the seismic models obtained, they enable us to identify a low-speed segment to the south and west of the Kambalny Volcano at a qualitative level. Hydrothermal manifestations and a magmatic body in the upper crust may be related to it.

FUNDING

This work was supported by the Russian Science Foundation, project no. 20-17-00075, and the Ministry of Science and Higher Education, project no. 075-15-2021-628 "Geophysical Research, Monitoring, and Forecasting of the Development of Catastrophic Geodynamic Processes in the Far East of Russia."

CONFLICT OF INTEREST

The authors declare that they have no conflicts of interest.

REFERENCES

1. O. A. Girina, D. V. Mel'nikov, A. G. Manevich, and A. A. Nuzhdaev, Sovrem. Probl. Distantsionnogo Zondirovaniya Zemli Kosmosa **14** (2), 263–267 (2017).
2. V. I. Levina, P. P. Firstov, and V. M. Zobin, Vulkanol. Seismol., No. 2, 81–98 (1980).
3. E. G. Kalacheva, S. N. Rychagov, G. P. Koroleva, and A. A. Nuzhdaev, J. Volcanol. Seismol. **10** (3), 188–203 (2016).
4. S. N. Rychagov, E. I. Sandimirova, A. V. Sergeeva, and I. A. Nuzhdaev, Vestn. Kamchatskoi Reg. Assots. Uchebn.-Nauchn. Tsentra Nauki Zemle, No. 4, Issue 36, 13–27 (2017).
5. S. L. Senyukov, I. N. Nuzhdina, S. Ya. Droznina, T. Yu. Kozhevnikova, Z. A. Nazarova, O. V. Sobolevskaya, A. N. Dolzhikova, et al., in *Russian Far East: Problems of Geophysical Complex Monitoring* (2017), pp. 73–77 [in Russian].
6. *Structure of Hydrothermal System,* Ed. by V. I. Belousov and I. S. Lomonosov (Nauka, Moscow, 1993) [in Russian].
7. V. M. Sugrobov, G. A. Karpov, and S. N. Rychagov, in *Proc. Scientific Conference Dedicated to Volcanologist Day in Institute of Volcanology and Seismology Far Eastern Branch RAS "Volcanism and Related Processes"* (Petropavlovsk-Kamchatskii, 2016). http://kcs.dvo.ru/ivs/publication/volc_day/2016/art52.pdf.
8. V. L. Syvorotkin, in *Structure of Hydrrothermal System,* Ed. by V. I. Belousov and I. S. Lomonosov (Nauka, Moscow, 1993), pp. 19–38 [in Russian].
9. F. Ardhuin, L. Gualtieri, and E. Stutzmann, in *Seismic Ambient Noise,* Ed. by N. Nakata, L. Gualtieri, and A. Fichtner (Cambridge Univ. Press, 2019).
10. G. D. Bensen, M. H. Ritzwoller, M. P. Barmin, A. L. Levshin, F. Lin, M. P. Moschetti, N. M. Shapiro, and Y. Yang, Geophys. J. Int. **169**, 1239–1260 (2007).
11. F. Brenguier, N. M. Shapiro, M. Campillo, A. Nercessian, and V. Ferrazzini, Geophys. Rev. Lett. **34**, L02305 (2007). https://doi.org/10.1029/2006GL028586
12. P. Gouédard, L. Stehly, F. Brenguier, M. Campillo, Y. Colin De Verdière, E. Larose, L. Margerin, P. Roux, F. J. Sánchez-Sesma, N. M. Shapiro, and R. L. Weaver, Geophys. Prospect. **56**, 375–393 (2008).
13. K. Jaxybulatov, N. M. Shapiro, I. Koulakov, A. Mordret, M. Landès, and C. Sens-Schönfelder, Science **346**, 617 (2014). https://doi.org/10.1126/science.1258582
14. A. L. Levshin, T. B. Yanovskaya, A. V. Lander, B. G. Bukchin, M. P. Barmin, L. I. Ratnikova, and E. N. Its, in *Seismic Surface Waves in a Laterally Inhomogeneous Earth,* Ed. by V. I. Keilis-Borok (Springer, Dordrecht, 1989), p. 304.
15. A. Mordret, D. Rivet, M. Landès, and N. M. Shapiro, J. Geophys. Res. Solid Earth **120** (1), 406–427 (2017). https://doi.org/10.1002/2014JB011654
16. N. Nakata and K. Nishida, in Seismic Ambient Noise, Ed. by N. Nakata, L. Gualtieri, and A. Fichtner (2019), pp. 239–266. https://doi.org/10.1017/9781108264808.010
17. I. Y. Koulakov, G. Maksotova, K. Jaxybulatov, E. Kasatkina, N. M. Shapiro, B. G. Luehr, S. El Khrepy, and N. Al-Arifi, Geochem., Geophys., Geosyst. **17** (10), 4195–4211 (2016).
18. V. V. Ponomareva, I. V. Melekestsev, and O. V. Dirksen, J. Volcanol. Geotherm. Res. **158** (1–2), 117–138 (2006).
19. N. M. Shapiro, M. Campillo, L. Stehly, and M. H. Ritzwoller, Science **307**, 1615–1618 (2005).
20. N. M. Shapiro, in *Seismic Ambient Noise,* Ed. by N. Nakata, L. Gualtieri, and A. Fichtner (Cambridge Univ. Press, 2019).

Translated by I. Bel'chenko